

Detailed characterization of South African high mineral matter inertinite-rich coals and density fractions and effect on reaction rates with carbon dioxide: Macerals, microlithotypes, carbominerites and minerals.

Raymond Everson^{a*}, Andrei Koekemoer^{a,b}, John Bunt^{a,b}, Hein Neomagus^a and Christopher Schwarz^c

^a School of Chemical and Minerals Engineering, North-West University, Potchefstroom Campus, Private Bag X6001, Potchefstroom, 2520, South Africa,

^b Sasol Technology (Pty) Ltd, P.O. Box 1, Sasolburg, 1947, South Africa.

^c Department for Energy Process Engineering and Chemical Engineering, TU Bergakademie Freiberg, Fuchsmühlenweg 9, Haus 1, 09596 Freiberg, Germany.

Keywords: South African Coals, Density fractions, Macerals, Minerals, Reactions rates

Abstract—An investigation was undertaken to determine the distribution of macerals and minerals in South African Highveld coal deposits as well as density fractions derived from a typical deposit. The corresponding effects on carbon dioxide gasification reaction rates were also studied. Detailed chemical, petrographic and mineral analyses, followed by reactivity measurements and reaction rate modeling were carried out. Coal samples from seven different coal mines and five density separated coal fractions ($<1.4 \text{ g.cm}^{-3}$ to $>2.0 \text{ g.cm}^{-3}$) were examined. It was found that the coal samples have ash contents in the range 21.6 to 38.8 wt. % and inertinite composition in the range 68 to 84 vol. %. The inertinites consist of high concentrations of semifusinites and inertodetrinite which is characteristic of South African Highveld coal deposits. The distribution of macerals and minerals in the different density fractions revealed high concentrations of inert detrinite, carbominerite and ash in the dense fraction. The presence of carbominerites was also found to increase with mineral content within the density range of 1.4 g.cm^{-3} to 1.8 g.cm^{-3} . The random pore model described the gasification reactivity very well with an increasing intrinsic reaction rate correlating with an increasing density of the coal which is attributed to an increasing pre-exponential factor.

INTRODUCTION

It is acknowledged that a detailed petrographic analysis and characterization of the associated properties of coals would be required for predicting combustion and gasification behaviour, particularly at temperatures below 1100°C (Cloke *et al.*, 1994). For this purpose, the identification and concentration of all the mono-macerals, bi-macerals, tri macerals and carbominerites which can consist of all possible forms of the macerals (reactive and non-reactive) and minerals should be determined. This is important since even low reflecting inertinites have been shown to be chemically reactive under combustion conditions (Cloke *et al.*, 1994; Borrego *et al.*, 1997; Choudhury *et al.*, 2007) and the composition of different mineral-maceral associations, (especially with high mineral matter containing coals) must be considered in such an analysis. This would be applicable to especially South African coal deposits originating in the Highveld Coalfield (Hagelskamp *et al.*, 1988; Snyman & Botha, 1993; Van Niekerk *et al.*, 2008; Falcon & Ham, 1988) and many coal deposits occurring in India (Choudhury *et al.*, 2007 Rajaram, 1999) where there are large reserves of high mineral matter and inertinite-rich coals which are currently used by major industrial consumers. It has been reported that coals from the Highveld region can consist of reactive semifusinites up to 60 vol.% (daf), with high mineral matter contents up to 30 wt. % (Van Niekerk *et al.*, 2008).

It has been shown that a batch of fine coal can consist of pure organic particles, pure mineral particles (excluded minerals) and particles consisting of mixtures of organic material and minerals (included minerals) with different compositions (Lui *et al.*, 2005; Everson *et al.*, 2008a) The distribution of macerals and minerals in different density fractions and the influence on reactivity has been examined and reported in the literature (Gilfillan *et al.*, 1999; Méndez *et al.*, 1999; Méndez *et al.*, 2003). Since the pure maceral groups have densities increasing as liptinite<vitrinite<inertinite, separation will occur with the heaviest fraction consisting of mostly

inertinites and the lightest fractions consisting of liptinites and vitrinites. The different minerals and carbominerites (such as carbo-silicates and carbankerite) with different densities (e.g. clays >dolomite) will also be distributed between the different fractions according to respective densities. Méndez *et al.*, (2003) who considered different density fractions obtained from vitrinite-rich coal, reported a favourable effect of minerals (high density fractions) on the combustion reactivity and related this to the macerals and the intimate association of organic/mineral phases present. Minerals consisting of calcium, iron, sodium and potassium are well known to exhibit catalytic activity, the effect of which can be significant for high ash coal fractions (Hashimoto *et al.*, 1986; Nishiyama, Y, 1986; Kyotani *et al.*, 1993; Huttinger and Natterman, 1994; Ye *et al.*, 1998; Zong *et al.*, 2007). The catalytic effect of inherent minerals has not been examined in-depth for different density fractions as evident from the literature. The gasification of chars with carbon dioxide only has been used by many researchers as a convenient reaction for estimating relative reactivities of chars since the rate of the reaction is such that the overall reaction is controlled by the chemical reaction at temperatures below 900° C (Liu *et al.*, 2000; Everson *et al.*, 2008a) Thermogravimetric analysis has been found to be appropriate for determining reactive properties (Russell *et al.*, 1998) since diffusion effects can be minimized by particle size and gas flowrates, and has been used extensively (Liu *et al.*, 2000; Everson *et al.*, 2008a; Lu *et al.*, 1992). Reaction rate modeling using experimental conversion results is considered to be the most suitable method for reaction rate assessment, provided a suitable model has been developed and evaluated. Overall reaction rate models incorporating structural effects in addition to the intrinsic kinetics have been evaluated, which include the Shrinking Core model (SCM) and Capillary/Random Pore Models (RPM) models. The Shrinking Core Model has a structural factor (Szekely *et al.*, 1976) depending only on the initial char properties (surface area and porosity), whereas the Random Pore Model (Bhatia & Perlmutter, 1980) accounts for surface area variations during reaction and is considered to be a more accurate model, but requires more coal related data.

An investigation was undertaken to determine the properties of some South African high mineral matter containing inertinite-rich coals and the effect of the ash and inertinite content on the carbon dioxide gasification reaction kinetics This paper presents (1) detailed characterization of seven typical high ash inertinite-rich South African coals in order to show the uniqueness with respect to the inertinite content and maceral-mineral associations, (2) detailed characterization of five different density fractions derived from a typical high mineral matter containing inertinite-rich coal, to demonstrate the distribution of macerals and minerals between the different fractions, (3) experimental reactivity results with carbon dioxide of the density fractions, and (4) results demonstrating the validity of the random pore model with associated parameters characteristic of the properties of the coal samples.

EXPERIMENTAL

Origin of coal samples

The coals examined originate from the South African Highveld coal fields which are currently used in large quantities for power generation and production of liquid fuels and chemicals. These bituminous coals have high concentrations of mineral matter and inertinite and are used in pulverized fuel combustors and moving bed gasifiers using lump coal. Seven run-of-mine coal samples from different sites (A to G) and five different density fractions (B1 to B5) derived from a typical parent coal (B) were examined.

Preparation of density fractions

The ROM coal samples (parent coals) were crushed to a particle diameter of (-1.7mm +1.0mm) and appropriate samples taken for detailed characterization. This particle size range was chosen to correspond to particle sizes used in fluidized bed gasification. The procedure for obtaining density fractions consisted of the separation of approximately 2 kg of the parent coal (B) using the float-sink method with mixtures of toluene (0.87 g.cm⁻³) and tetra-bromo-ethane (2.96 g.cm⁻³) as dense media (ISO 7936). The range of densities were between 1.4 g.cm⁻³ and 2.0 g.cm⁻³ and the five fractions produced were labelled as follows: B1- floats at 1.4 g.cm⁻³; B2 -sinks at 1.4 g.cm⁻³ floats at 1.6 g.cm⁻³ ; B3- sinks at 1.6 g.cm⁻³ floats at 1.8 g.cm⁻³ ; B4- sinks at 1.8 g.cm⁻³ floats at 2.0 g.cm⁻³ ; and B5-sinks at 2.0 g.cm⁻³ . After the separation, the particles were washed with distilled water and placed in a vacuum furnace at 60 °C for two hours to dry. A couple of scans were done on the particles using the scanning electron microscope (SEM) to check whether the separation media had been removed and it was found that no traces of chemicals were present on the coal particle surfaces. Several investigators. (Gilfillan *et al.*, 1999; Kawashima *et al.*, 2000; Wagner *et al.*, 2008; Strezof *et al.*, 2005) have confirmed the suitability of the chemicals used for laboratory-studies.

Characterization procedures

The proximate analysis of the parent coals and density fractions were characterized according to standard procedures as listed in Table 1. The maceral content of the coals was determined according to the procedure described in ISO 7404-3 by laboratories at Petrographics SA and the University of the Witwatersrand. The surface areas were determined by means of carbon dioxide (0°C) adsorption using a Micrometrics ASAP 2010 analyzer. Initially the samples were degassed at 25°C for a period of 48 hours. All of the gas adsorption experiments were done using a saturation pressure of 660 mm Hg. For the identification of the mineral constituents, XRD and QEMSCAN analysis were conducted on the coal and density fractions by XRD Analytical and Consulting Laboratories and Eskom: Sustainability and Innovation. The XRD analysis samples were prepared using a back loading preparation method by XRD Analytical Technology using a PANalytical X'Pert Pro powder diffractometer, with X'Celerator detector and variable divergence- and receiving slits with Fe filtered Co-K α radiation. For quantification purposes (wt. %), the Rietveld method was used in conjunction with Autopan software. The mineral components were also assessed by use of QEMSCAN an advanced SEM technique. (Quantification of minerals by scanning electron microscope). QEMSCAN analysis samples were prepared by mixing the coal particles with molten carnauba wax in a 30mm mould and allowing this to cure. This solid wax block was then polished, exposing the individual particles in cross-section. Polished blocks were analyzed by positioning the scanning electron beam at predefined points across a particle. At each point a 7 millisecond, 1000 count X-ray spectrum was acquired and the elemental proportions were used to identify the mineral phases at each point. This analysis is a specialized application SEM analysis, where a backscattered electron image (BSI) is obtained. This BSI is an atomic-weight contrast image, which allows for the elemental composition of the coal to be evaluated by means of image processing procedures; as the high molecular-weight elements appear brighter compared to the low molecular-weight elements. This also allows distinguishing between the association of minerals and macerals, as the minerals are observed as bright areas on the SEM micro-photographs, while the carbon-rich macerals are seen as dull areas.

Reactivity studies

Gasification results of the five density separated fractions were obtained using a thermogravimetric analyzer (TGA) operating at atmospheric pressure (87.5 kPa), and at four reaction temperatures (between 1000°C and 1070°C). The TGA used was a Thermax 700 model supplied by the Cahn Company. The reactor consisted of a perforated platinum basket suspended from a micro balance with a movable concentric oven and capable of attaining a temperature of 1200°C. A sample mass of coal equivalent to approximately 500 mg (screened to a particle diameter of -1140 μm +1000 μm) was loaded into the basket. A gas flow rate of 200 $\text{ml}\cdot\text{min}^{-1}$ was used throughout the experimental period which was established to be suitable for the elimination of gas film diffusion around the coal particles. The experimental procedure consisted of pyrolysis in the presence of nitrogen and gasification with pure carbon dioxide. This was achieved by heating the reactor at a rate of 30°C per minute to a temperature of 1000°C in the presence of pure nitrogen, followed by an isothermal period at this temperature and flowing nitrogen until a constant mass was obtained, which indicate the completion of the pyrolysis period. Pure carbon dioxide was then introduced into the reactor and the gasification reaction continued until complete conversion of all the carbon containing compounds with only mineral remaining in the basket. The gases used were of high purity and supplied by African Oxygen (Afrox) limited South Africa

RESULTS AND DISCUSSION

Proximate Analysis and Physical Properties.

Results consisting of proximate analysis together with gross calorific values for the parent coals and density fractions (derived from parent coal B) are shown in Table 1. The air-dried ash content of the parent coals vary between 21.6 and 38.8 wt. %, with gross calorific values ranging between 17.4 and 23.0 $\text{MJ}\cdot\text{kg}^{-1}$ (air-dry basis) which is characteristic of South African Highveld coals (Hagelskamp *et al.*, 1988; Snyman & Botha, 1993; Van Niekerk *et al.*, 2008; Falcon & Ham, 1988; Engelbrecht *et al.*, 2011). The results obtained are also very similar to properties of most of the Indian coals which can have ash contents greater than 45.0 wt. % (Choudhury *et al.*, 2007; Falcon & Ham, 1988). The distribution of ash, volatile matter and fixed carbon between the different density fractions is as expected, which is attributed to the mineral matter and mineral matter-carbon associations having a higher density than the carbon-containing structures. This result has been reported by numerous investigators for different high ash coal samples (Méndez *et al.*, 1999; Méndez *et al.*, 2003). It should be noted

that the high density fraction (B5) contains significantly more sulphur as a result of the increased content of sulphur-bearing minerals such as pyrite in the more dense coal fractions (see Table 1). The specific surface areas of the density fractions using carbon dioxide adsorption are also shown in Table 1. For the density fractions, the micro-pore surface area increases with decreasing density, which is to be expected as the lighter fractions contain more fixed carbon and less minerals.

Table 1. Proximate analysis and surface areas of coals and density fractions.

	Coal samples							Density fractions derived from Coal B				
	A	B	C	D	E	F	G	B5	B4	B3	B2	B1
Proximate analysis (air dry wt. %) (ISO 562, ISO 1171 and SABS.SM 924)												
Moisture	6.4	4.8	4.4	4.2	3.7	4.5	5.3	2.1	3.1	3.3	3.7	4.0
Volatile Matter	22.2	20.3	23.1	19.3	18.7	23.5	21.1	14.5	16.9	19.0	22.1	27.0
Fixed Carbon	49.8	48.1	49.9	42.5	38.8	53.4	49.5	10.4	28.0	41.5	55.2	60.1
Ash	21.6	26.8	22.6	34	38.8	18.6	24.1	73.0	52.0	36.2	19.0	8.9
Sulphur	1.2	1.3	1.2	3.5	1.8	1.1	1.1	15.4	3.2	1.4	0.7	0.8
Calorific Values (air dry wt.%)												
Gross MJ.kg ⁻¹	21.8	17.5	20.5	19.4	17.4	23.0	21.1	3.3	9.8	16.6	23.5	28.3
Surface Areas												
^a Surface area S _{CO2} (m ² .g ⁻¹)	152	117	120	137	123	146	154	38	65	102	138	142
^b Porosity (%)	-	-	-	-	-	-	-	12.5	17.6	11.2	14.9	14.7
^b Bulk density (g/cm ³)	-	-	-	-	-	-	-	2.21	1.69	1.675	1.42	1.25

^a : carbon dioxide adsorption (Dubinin Radushkevich method); - : not determined; ^b : Mercury Intrusion

Petrographic analysis

The results obtained from the petrographic analysis of the coal samples and the density separated coal fractions are shown in Table 2 which includes the maceral, microlithotype and carbominerite compositions.

Table 2. Maceral content of coal samples (Mineral matter free, vol.%).

Maceral group	Coal samples							Density fractions derived from coal B				
	A	B	C	D	E	F	G	B5	B4	B3	B2	B1
Vitrinite	23	23	23	14	21	29	22	11	8	5	9	32
Liptinite	5	4	3	2	4	3	4	3	< 1	3	7	5
Total inertinites	72	73	74	84	75	68	74	86	92	92	84	63
- Reactive Semifusinites	13	15	13	15	13	9	13	0	3	1	3	8
- Inert Semifusinites	23	21	20	25	20	17	19	11	11	20	35	33
Total Semifusinites	36	36	33	40	33	26	32	11	14	22	38	41
- Fusinite	3	3	4	2	2	2	3	0	2	< 1	3	3
- Micrinite	1	1	2	1	2	2	2	0	0	0	1	< 1
- Reactive Inertodetrinite	8	10	11	13	10	12	12	0	0	< 1	3	2
- Inert Inertodetrinite	24	23	24	28	28	26	25	75	76	69	40	16
Total Inertodetrinite	32	33	35	41	38	38	27	75	76	70	42	18
Mean Random Reflectance RoV	0.59	0.64	0.63	0.64	0.61	0.61	0.63	-	-	-	-	-

Maceral analysis:

Coal samples

The distribution of the macerals in the parent coals is characterized by a high proportion (68% to 84%) of inertinite, consisting of 26% to 40% semifusinite and 32% to 41% inertodetrinite respectively. The inertodetrinite consists of mainly inert inertodetrinite 17% to 25% as opposed to 9% to 15% reactive inertodetrinite. The presence of such high concentrations of inertodetrinite together with a high ash concentration appears to be a unique property of South African Highveld coals currently used in large quantities for power generation (pf combustion) and liquid fuel production (gasification). It should be noted that the concentration of liptinite is very low. A comparison with some coals available in India (Choudhury *et al.*, 2007) is shown in Figure 1, which indicates that the Indian coals have slightly higher concentrations of semifusinites, but with much lower concentrations of inertodetrinite. The parent coals mean random reflectance of vitrinite are in the order of 0.59 to 0.64 and calorific values range between 17.4 and 21.8 MJ/kg (air-dry basis) which classifies the coal as bituminous grade C coals.

Density Fractions

A detailed analysis of all macerals occurring in the different density fractions are shown in Table 2 and Figures 2 and 3. The distribution of macerals amongst the different density fractions reveals that only the inert inertodetrinite increases with the density of the fractions, whilst all the other inertinites, vitrinites and liptinites tend to increase with decreasing density. The segregation of the vitrinites and liptinites in the low density

fractions is as a result of the low densities of these pure macerals, whilst the inertinites (other than inert inertodetrinite) which have higher densities (Méndez *et al.*, 2003) behave in an abnormal manner. This latter behaviour can be attributed to associations of the inertinites with vitrinites (microlithotypes) with a resultant lower density. The inert inertodetrinite can also be associated with the minerals (carbominerites) having an increased density and causing the inert inertodetrinite to occur in high density fractions. The presence of a large concentration of inert inertodetrinite and ash which increases with density is considered to be a unique property of the coals deposits occurring in the South African Highveld region.

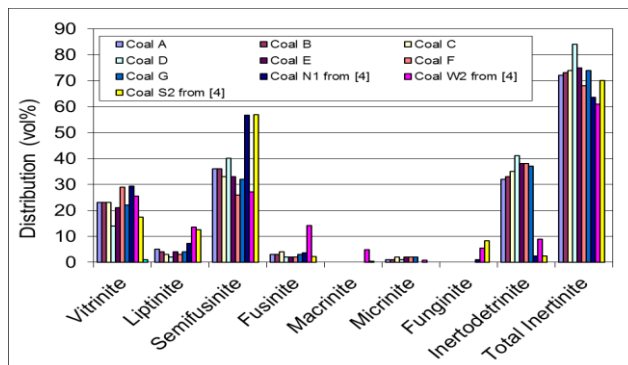


Figure 1: Comparison of macerals in parent coals with coals occurring in India. (A to G are coals used in this investigation and N1,W2 and S2 are results reported by Choudhury *et al.*, 2007).

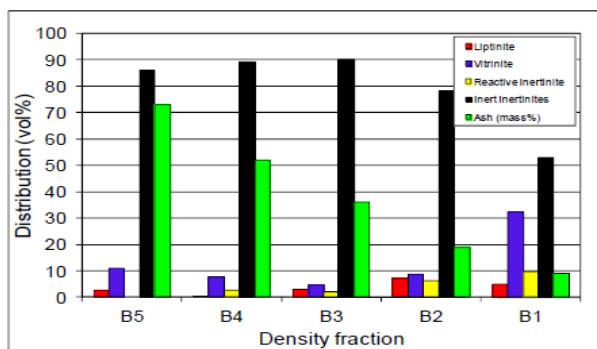


Figure 2: Distribution of macerals and ash in density fractions.

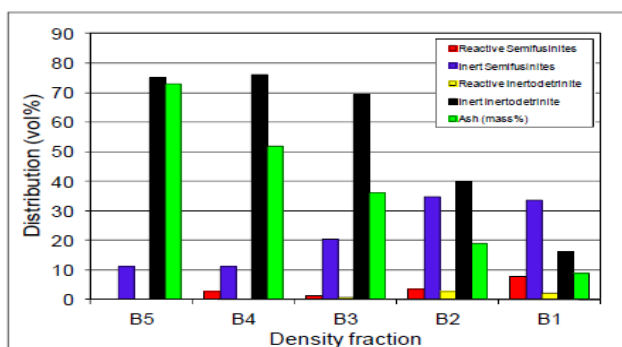


Figure 3: Distribution of Semifusinites, Inertodetrinite and Ash in density fractions

Microlithotype analysis:

The results obtained from the microlithotype evaluation of the parent coals and density fractions are shown in Table 3, which includes the mono-macerals, intermediates, carbominerites and minerite groups.

Table 3. Microlithotype content of coal samples (Mineral matter basis, vol. %)

	Coal samples							Density fractions derived from Coal B				
	A	B	C	D	E	F	G	B5	B4	B3	B2	B1
Mono-macerals												
Vitrinite	9	9	5	7	5	10	5	<1	3	2	4	19
Liptinite	0	0	0	0	0	0	0	0	0	0	0	<1
Inertite	41	36	40	38	32	40	40	5	47	73	68	47
Total Mono-macerals	50	45	45	45	37	50	45	6	50	75	73	67
Intermediates												
Vitrinerite	10	13	10	11	9	12	10	0	3	2	9	12
Clarite	2	1	2	2	1	2	1	0	<1	<1	<1	2
Durite	9	6	6	6	7	5	9	0	<1	3	6	4
Tri-macerite	9	9	8	7	9	8	6	<1	<1	2	3	8
Total Intermediates	30	29	26	26	26	27	26	<1	4	8	18	26
Carbominerites												
C-Arg& C-Sil	9	9	13	12	16	14	14	6	32	11	4	<1
Carbo-pyrite	2	3	3	2	2	1	2	2	3	<1	<1	<1
Carbankerite	4	4	1	4	5	2	4	<1	1	4	5	4
Total Carbominerites	15	16	17	18	23	17	20	9	36	16	10	5
Minerite	5	10	12	11	14	6	9	85	11	2	<1	1

Coal Samples

The mono-maceral group consisting mainly of inertite (32 to 40 vol.%) contributes between 45% and 50% of the total microlithotypes, while the intermediate fraction amounts to 26% to 30% with inertinite spread between vitrinite, durite and trimacerite. The presence of these intermediates causes the occurrence of inertinites in the low density fractions. The carbominerite groups amount to 15% to 23% of the total coal, while the mineral rich minerite groups (> 60% mineral matter) are much less, with the concentrations ranging from 5% to 14%. The main contribution to the carbominerite content of the coals is from the carb-argillite and carbo-silicate groups, which are the clay and quartz-containing groups, while the second largest contribution is made by the carbonate-containing carb-ankerite group. The same trend can be seen for the minerite groups in the carbominerite groups, with the bulk of the minerite content consisting of clay and quartz groups. The carbonate groups have the second most significant contribution to the minerite content of the coals, and again it can be seen that the pyrite group contributes the least amount to the mineral content of the coals.

Density Fractions

The inertite mono-maceral group makes up the bulk of the microlithotypes in each fraction, except for the mineral-rich fraction (B5). The inertite content concentrates towards the heavier density fractions, reaching a peak in the B3 and B2 fractions. The vitrinite mono-maceral is mainly found in the lowest density fraction, with minor inclusions in the other 4 fractions. The intermediate groups consisting of maceral-maceral associations show a steady decrease from the lightest to the heaviest fraction. The most prominent intermediate group was found to be the combined vitrinite and inertinite containing group known as vitrinite.

The carbominerite groups, referring to the maceral-mineral associations (5 to 60 vol. %) minerals) show a steady increase from the lightest to the heaviest fraction, but then drops in the most dense fractions. This again shows the tendency of the mineral groups to concentrate towards the heavy density fractions. The minerite groups increase from the lightest to the heaviest density fractions, with an almost exponential increase observed into these heavy fractions, as most of the mineral matter is concentrated in these fractions.

Overall it can be concluded that there is an increase in mineral-containing groups from the lightest to the heaviest density fractions, while the opposite trend is observed for the mono-maceral and intermediate groups. This shows the effectiveness of density separation to segregate and concentrate mineral and organic matter into separate fractions.

The carb-argillite and carbo-silicate groups make up the bulk of the total carbominerite content and the combined carb-argillite and carbo-silicate groups increase towards the dense fractions, reaching a peak in the B4 density fraction. The same trend is observed for carbo-pyrite. Carb-ankerite shows the opposite trend as it increases towards the less dense fractions, reaching a peak in the B2 fraction.

Mineral analysis

Coal Samples

The composition of the major minerals (>10%) and pyrite in the coal are reported in Table 4 as determined by XRD. The most abundant minerals are the clays consisting mainly of kaolinite, followed by quartz and then the carbonates consisting of a large fraction of dolomite (Matjie & Van Alphen, 2008; Van Dyk *et al.*, 2009; Bunt *et al.*, 2011). The pyrite content has a maximum value of 2.9% which agrees with the findings of Matjie & Van Alphen (2008).

Table 4: Minerals analysis of parent coals (Mineral matter base, wt. %).

Minerals	A	B	C	D	E	F	G
Total carbonates	17.1	13.6	9.1	13.4	10.5	15.1	14.6
- Calcite	2.4	2.5	1.2	2.0	1.8	2.6	1.7
- Dolomite	14.7	11.1	7.9	11.4	8.7	12.5	12.9
Clays	55.9	53.0	49.3	55.5	48.2	50.3	55.5
Quartz	20.8	25.3	32.6	25.2	22.5	17.0	23.4
Pyrite	0.5	2.7	2.9	0.5	1.2	1.2	0.6

Density Fractions

The mineral distributions between the different density fractions prepared from parent coal B as determined by QEMSCAN are shown in Table 5. The main components are again the clays (kaolinite, muscovite, illite) and quartz, which increase with the density of the fractions and the carbonates decreasing with density of the fractions. This behaviour is well known which is attributed to the density of the different minerals. The concentration of the clays and quartz in the more dense fractions agrees with the results from the carbominerite analysis, which also show that the carb-argillite and carbo-silicate groups to increase into the more dense fractions as shown in Table 4. Dolomite being a low density mineral (Oki *et al.*, 2004), which also contributes significantly to the total minerals content and which increases with decreasing fractional density, also agrees with the calcium-containing carb-ankerite groups shown in Table 4. Pyrite tends to increase towards the more dense fractions showing an almost exponential trend and correlates with the results from the carbominerite analysis, which found that the carbo-pyrite also increases towards the more dense fractions (Table 4). Pyrite has been examined by many researchers (Nishiyama, 1986; Kyotani *et al.*, 1993; Samaras *et al.*, 1996; Yücel *et al.*, 2007) who have found that this mineral, along with calcium, may act as catalyst in the gasification of coal. The calcite contained in the density fractions does not show any trend. For both coals the calcite reaches a maximum in the densest fraction. Rutile is a relatively high density mineral, as seen in its distribution towards the heavier density fractions. Apatite, also a calcium-containing mineral, is rarely observed in any of the fractions, with the largest concentrations seen in the less dense fractions. Siderite contributes the smallest amount to the total mineral content of the density fractions, as it was only found in the lowest dense fraction.

Table 5: Mineral distributions of density fractions (Mineral matter base, wt.%).

Mineral	B5	B4	B3	B2	B1
Alunite	3.8	5.1	12.0	14.0	12.0
Pyrite	8.2	3.3	1.5	0.9	0.9
Siderite	0	0	0	0	0.9
Calcite	6.0	1.8	2.4	3.1	4.3
Dolomite	2.0	2.5	10.5	32.5	31.6
Apatite	0.2	0.1	0	3.1	2.6
Kaolinite	50.1	57.0	40.2	23.7	23.1
Quartz	18.9	17.2	17.1	9.2	13.7
Illite	0.7	1.9	4.1	6.6	1.7
Muscovite	5.3	6.7	7.8	2.6	1.7
Microcline	1.4	0.6	1.5	1.3	0.9
Rutile	2.8	3.1	2.0	0.9	0.9
Other	0.5	0.4	1.0	2.2	5.1

Reactivity Results

The experimental results with carbon dioxide obtained from the thermogravimetric analyser consisting of weight loss versus time relationships were converted to carbon conversion versus time results on a mineral free basis (Everson *et al.* 2008b) in order to confine the reaction rate modeling to the carbon phase only. Typical results for the different density fractions are shown in Figure 4 which clearly indicates the effect of the different properties of the density fractions.

In order to accomplish a meaningful comparison, since there are many variables which can affect the reactivity, it was decided to evaluate the intrinsic reaction rate for the different char samples with a suitable reaction rate model. The advantage of using a model is that it is possible to account for the interrelationships of most of the variables. For this purpose a random pore model (reaction rate controlling) was chosen as it incorporates many of the properties of the chars examined as reported by Everson *et al.* (2008b) who examined very similar coal samples. This assumption was validated as shown below. A description of the random pore model (Bhatia & Perlmutter, 1999) and the method for validation and determination of reaction rate equation is given by Everson *et al.* (2008b). Briefly this consists of a step-wise regression method of evaluation of the unknown parameters ψ and r^L (equation (1)) which describes the structure behavior and lumped reaction kinetics respectively of the conversion process.

$$x = 1 \exp \left(-r^L t \left(1 + \frac{\psi r^L t}{4} \right) \right) \quad \text{(Fractional carbon conversion)} \quad (1)$$

$$\text{with } r^L = \frac{r s_0}{(1 - \varepsilon_0)} \quad \text{(Lumped reaction rate)} \quad (2)$$

$$\psi = \frac{4\pi L_o(1-\varepsilon_o)}{S_o^2} \quad (\text{Structural Parameter}) \quad (3)$$

$$r = k_o \exp\left(\frac{-E}{RT}\right) P_{\text{co}_2} \quad (\text{Intrinsic reaction rate}) \quad (4)$$

Using a normalized time variable ($t / t_{0.9}$) as shown in equation (5), which can be derived from equation (1) a convenient method was developed (Everson *et al.*, 2008b) to determine the structural parameter by regression from a plot of conversion versus the normalised time variable.

$$\frac{t}{t_{0.9}} = \frac{\sqrt{1-\psi} \ln(1-x) - 1}{\sqrt{1-\psi} \ln(1-0.9) - 1} \quad (\text{Normalised equation}) \quad (5)$$

A unified plot independent of temperature, pressure and gas composition will be obtained for a reaction controlled reaction system from which the structural parameter can be calculated by regression. With a known value of the structural parameter ψ , the lumped reaction rate r^L can be calculated by regression using equation (1) and consequently the intrinsic reaction rate (equation (2)) and the corresponding pre-exponential factors and activation energies (Arrhenius parameters) using equation (4). The Arrhenius parameters can be obtained from a plot of the logarithmic form of equation (4) which is a well-established technique. The power dependence of the partial pressure has been well established by many investigators (Everson *et al.*, 2008b) and was consequently assumed to be equal to 0.5 for all the calculations reported below. It was found that the random pore model with the parameters shown in Table 6 which were evaluated according to the procedure described above agrees very well with experimental results at atmospheric pressure (87.5 kPa) and at temperatures between 1000°C and 1070°C. Typical results are shown for all chars in Figure 4 for a temperature of 1000°C.

The structural parameter based on the initial properties of the chars (equation (3)) have values larger than 2 for B4 and B5 which indicates that the pores (diameter) in these chars initially increase followed by coalescence (overlapping pores) whereas with the structural parameters for B1, B2 and B3 show that pores coalesce only during the gasification reaction.

The intrinsic reaction rates (r) calculated from equation (5) with the regressed lumped reaction rate values (Table 6) and with the properties of the coal samples (ε_o, S_o) for the different char samples and temperatures are shown in Figure 5. A significant increase over the upper range of the density fractions ($>1.8 \text{ g.cm}^{-3}$) was obtained with the chars from coal with very high ash and high inertinite content (low total macerals). This was also observed by Mendez *et al.* [13] who reported results for high ash, vitrinite-rich, anthracite coals over the same density range as examined in this investigation. The reaction rate parameters consisting of the pre-exponential factors and activation energies were calculated using equation (5) and the results are shown in Table 6 and Figure 6. The activation energies do not change much for the different density samples indicating that no significant change in the catalytic effect of the minerals present in the different chars was detected. This means that the different mineral compositions did not have different catalytic properties (activation energy).

The pre-exponential factors however changed very much for all temperatures which contributed almost entirely to the variation of the intrinsic reaction rate, which can be explained in terms of the availability of active carbon sites in a carbon/mineral matrix. For the high density fractions (high mineral/maceral) there are active reaction sites present on an inertinite-rich carbon surface surrounded by a high concentration of minerals (more sites subject to catalytic effects). In the case of the low density fractions (low mineral/maceral) there are reactive sites on vitrinite rich surfaces surrounded by a low concentration of minerals (less sites subjected to catalytic effects). The inertinite present in the high density fraction was also shown to consist predominantly of inert inertodetrinite, characteristic of South African highveld coals.

Table 6: Regressed and calculated parameters for Random Pore Model.

	B1	B2	B3	B4	B5
Structural Parameter (regressed) ψ	1.0	1.0	1.9	2.9	2.9
Lumped Reaction Rate (regressed) r^L (s ⁻¹)					
Temperatures					
- 1000°C	1.7	1.5	1.4	1.5	2.7
- 1015°C	2.7	2.7	2.5	2.5	4.5
- 1030°C	3.2	2.8	2.6	3.1	4.8
- 1070°C	4.1	3.6	3.7	4.7	8.4
Activation Energy E (kJ/mole) (calculated)	174	163	190	194	199
Pre-exponential Factor k_0 (m/Pa ^{0.5} m) (calculated)	7.37x10 ¹⁰	2.19x10 ⁹	3.04x10 ¹⁰	7.09x10 ¹⁰	2.66x10 ¹¹

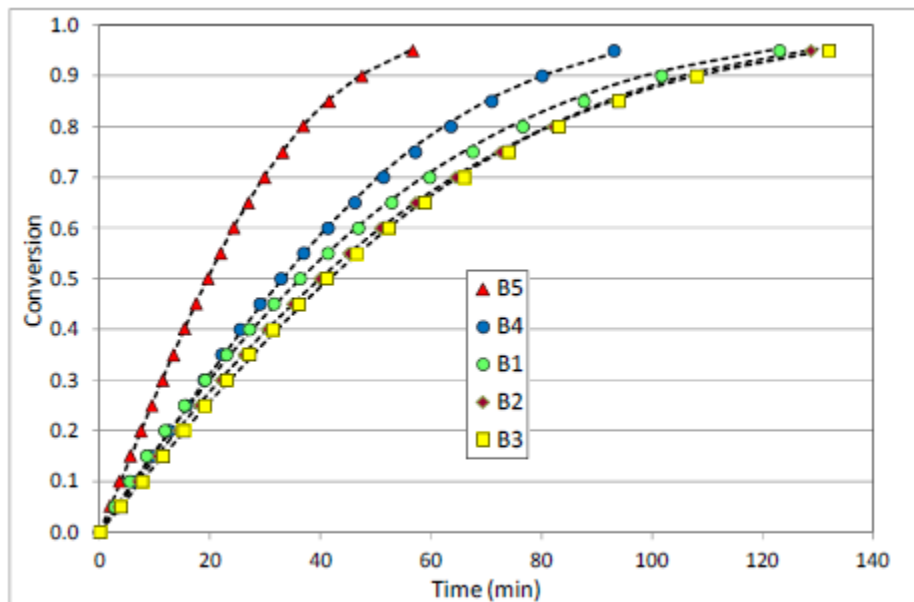


Figure 4. Experimental and modeling results at 1000°C (The symbols the experimental results and the dotted lines are the respective model predictions).

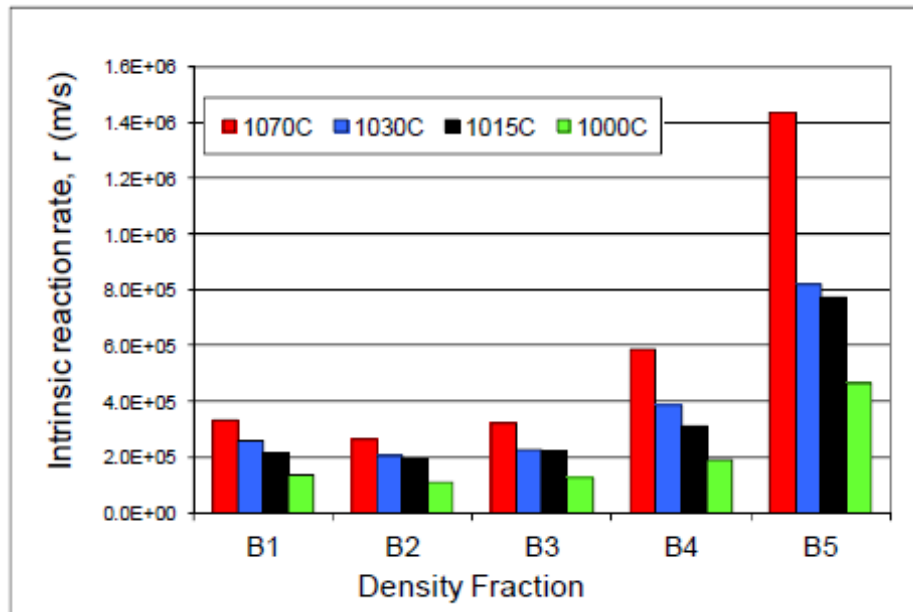


Figure 5: Intrinsic reaction rates of all the chars for different temperatures

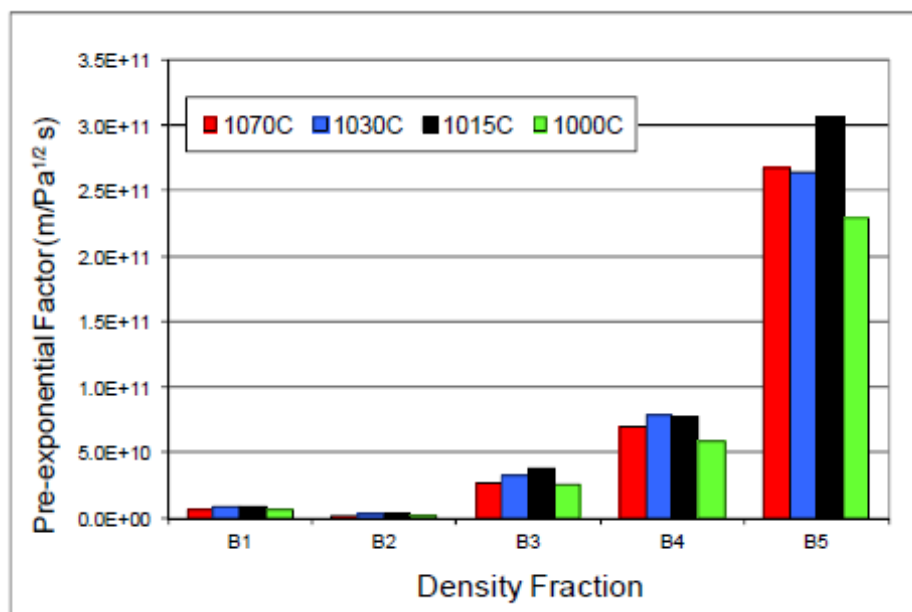


Figure 6: Pre-exponential factors for all the chars at different temperatures

CONCLUSIONS

Coal characterisation results showed that the distribution of macerals in the parent coals is characterized by a high proportion (68% to 84%) of inertinite, consisting of 26% to 40% semifusinite and 32% to 41% inertodetrinite respectively. The inertodetrinite consists of mainly inert inertodetrinite 17% to 25% as opposed to 9% to 15% reactive inertodetrinite. The presence of such high concentrations of inertodetrinite together with a

high mineral matter concentration appears to be a unique property of South African Highveld coals currently used in large quantities for power generation (pf combustion) and liquid fuel production (gasification). The distribution of macerals amongst the different density fractions revealed that only the inert inertodetrinite increases with the density of the fractions. The segregation of the vitrinites and liptinites in the low density fraction is as a result of the low densities of these pure macerals, whilst the inertinites (other than inert inertodetrinite) which have higher densities behave in an abnormal manner. This latter behaviour can be attributed to associations of the inertinites with vitrinites (microlithotypes) with a resultant lower density. The inert inertodetrinite can also be associated with the minerals (carbominerites) having an increased density and causing the inert inertodetrinite to occur in high density fractions.

The intermediate groups consisting of maceral-maceral associations showed a steady decrease from the lightest to the heaviest fraction. The volatile matter content correlates with the intermediates content of the coal fractions; as an increase in the intermediate groups lead to increased volatile matter content. The most prominent intermediate group was found to be the combined vitrinite and inertinite containing group known as vitrinertite. Overall it can be concluded that there is an increase in mineral-containing groups from the lightest to the heaviest density fractions, while the opposite trend is observed for the monomaceral and intermediate groups. This shows the effectiveness of density separation to segregate and concentrate mineral and organic matter into separate fractions.

The random pore model with chemical reaction controlling was found to describe the reaction kinetics of the chars from the different density fractions with carbon dioxide very well. The chars from the high density coal fractions (high minerals low macerals) experienced an initial growth period followed by a collapsing period of the pores. Intrinsic reaction rates were evaluated from the model and it was found that this increased most significantly over the high densities range. From an evaluation of reaction rate parameters it was found that the different minerals/maceral compositions of the different density fractions did not affect the activation energy but has a pronounced effect on the pre-exponential factor. It was concluded that with increasing density (with more minerals and inertinites) that the active carbon sites/minerals was the determining affect. Thus, high density particles are more reactive, but with a lower loading of carbon.

NOTATION

E	activation energy kJ/mole
k_0	pre-exponential factor, $m/Pa^{0.5} s$
L_o	total pore length per unit volume, $m m^{-3}$
n	power dependence of carbon dioxide pressure
P	CO ₂ partial pressure of carbon dioxide, Pa
R	universal gas constant, kJ mole ⁻¹ K ⁻¹
r	intrinsic reaction rate, $m s^{-1}$
r^L	lumped reaction rate at surface S^{-1}
S_o	initial surface area, $m^2 m^{-3}$
T	temperature, K
t	time, s
$t_{0.9}$	time for 90% carbon conversion, s
X	fractional conversion of carbon.

Greek Letters

ϵ_o	initial voidage
Y	structural parameter

REFERENCES

1. Bhatia, SK & Perlmutter, DD 1980, 'A random pore model for fluid-solid reactions: I. Isothermal kinetic control', *American Institute of Chemical Engineering Journal*, vol. 26, no.3, pp. 379:385.

2. Borrego, AG, Alvarez, D & Menendez, R 1997, 'Effects of inertinite content in Coal on Char Structure and combustion', *Energy Fuels*, vol. 43, pp. 702-708.
3. Bunt, JR, Waanders, FB & Schobert, H 2011, 'Behaviour of selected major elements during fixed-bed gasification of South African bituminous coal', *J.Anal.Appl.Pyrol.*, vol. 93, pp. 85 -94.
4. Choudhury, N, Boral, P, Mitra, T, Adal, AK, Choudhury, A & Sarkar, P 2007, 'Assessment of the nature and distribution of inertinite in Indian coals for burning characteristics', *International Journal of Coal geology*, vol. 72, pp. 41-152.
5. Cloke, M & Lester, E 1994, 'Characterization of coals for combustion using petrographic analysis: A review', *Fuel*, Vol 73, no. 3, pp. 315-320.
6. Engelbrecht, AD, Everson, RC, Neomagus, HWJP & North, BC 2011, 'Fluidized bed gasification of selected South African coals', *Journal of the South African Institute of Mining and Metallurgy*. vol. 10, pp. 225-230.
7. Everson, RC, Neomagus, HWJP, Kaitano, R, Falcon, R & Du Cann, VM 2008a, 'Properties of high ash coal-char particles derived from inertinite-rich coal: I. Chemical, structural and petrographic characteristics', *Fuel*, vol. 87, pp. 3082-3090.
8. Everson, RC, Neomagus, HWJP, Kaitano, R, Falcon, R, Van Alphen, C & Du Cann, VM 2008b, 'Properties of high ash coal-char particles derived from inertinite-rich coal: II Gasification kinetics with carbon dioxide', *Fuel*, vol. 87, pp. 3403-3408.
9. Falcon, R & Ham, AJ 1999, 'The characteristics of Southern African coals', *Journal of the South African Institute of Mining and Metallurgy*, vol. 88, no.5, pp. 145-161.
10. Gilfillan, A, Lester, E, Cloke, M & Snape, C 1999, 'The structure and reactivity of density separated coal fractions', *Fuel*, vol. 78, pp. 1639-1644.
11. Hagelskamp, HHB & Snyman, CP 1988, 'On the origin of low-reflecting inertinites in coals from the Highveld coalfield, South Africa', *Fuel*, vol. 67, pp. 307-313.
12. Hashimoto, K, Miura, K. & Ueda, T 1986, 'Correlation of gasification rates of various coals measured by rapid heating method in a steam atmosphere at relatively low temperature', *Fuel*, vol. 65, pp.1516-1523.
13. Hutterer, KJ & Natterman, C 1994, 'Correlation between coal reactivity and inorganic matter content for pressure gasification with steam and carbon dioxide', *Fuel*, vol. 73, pp. 1682-1684.
14. Kawashima, H, Yamashita, Y & Saito, I 2000, 'Studies on the structural changes of coal density-separated components during pyrolysis by means of solid-state C NMR spectra', *Journal of Analytical and Applied Pyrolysis*, vol.53, pp. 35-50
15. Kyotani, T, Kubota, K, Cao, J, Yamashita, H & Tomita, A 1993. 'Combustion and CO₂ gasification of coals in a wide temperature range', *Fuel Processing Technology*, vol. 36, pp. 209-217.
16. Liu, G, Benyon, P, Benfell, KE, Bryant, GW, Tate, AG, Boyd, RK, Harris, DJ & Wall, TF 2000, 'The porous structure of bituminous coal chars and its influence on combustion and gasification under Chemically controlled conditions', *Fuel*, vol. 79, pp. 617-626.
17. Lui, Y, Gupta, R, Sharma, A, Wall, T, Butcher, A, Miller, G, Gottlieb, P & French, D 2005, 'Mineral matter-organic matter association characterisation by QEMSCAN and application in coal utilization', *Fuel*, vol. 84, pp. 1259-1267.
18. Lu, GQ & Do, DD 1992, 'A kinetic study of coal reject-derived char activation with CO₂, H₂O and air', *Carbon*, vol. 30, no.1, pp. 21-29.
19. Matjie, RH & Van Alphen, C 2008, 'Mineralogical features of size and density fractions in Sasol coal gasification ash, South Africa and potential by-products', *Fuel*, vol. 87, pp. 1439-1445.
20. Méndez, LB, Borrego, AG, Alvarez, D, Tarazona, R, Menendez, R, Russell, NV, Wigley, F & Williamson, J 1999, 'The influence of coal mineral matter distribution on char structure and reactivity', *Proceeding of 10th ICCS, Taiyuan, China, Prospects for Coal Science in the 21st Century*. Editors: Li, BQ & Liu, ZY. Shanxi Science and Technology Press, pp.543-546.
21. Méndez, LB, Borrego, AG, Martínez-Tarazona, MR & Menendez, R 1999, 'Influence of petrographic and mineral matter composition of coal particles on their combustion reactivity', *Fuel*, vol. 82, , pp. 1875- 1882.

22. Nishiyama, Y 1986, Catalytic behaviour of iron and nickel in coal gasification. *Fuel*, vol. 65. no.10, pp.1404-1409.
23. Oki, T, Yotsumoto, H & Owada, S 2004, 'Calculation of degree of mineral matter liberation in coal from sink-float separation data', *Minerals Engineering*. vol. 17, pp. 39-51. Rajaram, S 1999, 'Next generation CFBC', *Chemical Engineering Science*, vol. 54, 5, pp. 565-5571.
Russell, NV, Beeley, TJ, Man, CK, Gibbins, JR & Williamson, J 1998, 'Development of TG
24. measurements of intrinsic char combustion reactivity for industrial and research purposes', *Fuel Processing Technology*, vol. 57, pp. 113-130.
25. Samaras, P, Diamadopoulos, E & Sakellariopoulos, G 1996, 'The effect of mineral matter and pyrolysis conditions on the gasification of Greek lignite by carbon dioxide', *Fuel*, vol. 75, pp. 1108-1114.
26. Snyman, C P & Botha, W J 1993, 'Coal in South Africa', *Journal of African Earth Sciences*, vol. 16, pp. 171-180.
27. Strezov, V, Lucas, JA & Wall, TF 2005, 'Effect of pressure on the swelling of density-separated coal particles', *Fuel*, vol. 84, pp. 1238-1245.
28. Szekely, J, Evans, JE & Sohn, HY 1976. *Gas-Solid Reactions*, Academic Press, London.
29. Van Dyk, JC, Benson, SA, Laumb, ML & Waanders, FB 2009. 'Coal and coal ash characteristics to understand mineral transformations and slag formation', *Fuel*, vol. 88, no. 6, p. 1057-1063.
30. Van Niekerk, D, Pugmire, RJ, Solum, MS., Painter, PC & Mathews, JP 2008, 'Structural
31. characterization of vitrinite-rich and inertinite-rich Permian-aged South African bituminous coals', *International Journal of Coal Geology*, vol. 76, pp. 290-300.
32. Wagner, NJ, Matjie, RH, Slaghuis, JH & Van Heerden, JHP 2008, 'Characterization of unburned carbon present in coarse gasification ash', *Fuel*, vol. 87, pp. 683-691.
33. Ye, DP, Agnew, JB & Zhang, DK 1998, 'Gasification of South Australian low rank coal with carbon dioxide and steam: Kinetics and reactivity studies', *Fuel*, vol. 77, pp. 1209-1219.
34. Yücel, H, Cakal, G.O. & Gürüz, A.G. 2007. 'Physical and chemical properties of Turkish lignites and their pyrolysis and gasification rates determined by thermogravimetric analysis', *Journal of Analytical and Applied Pyrolysis*, vol. 80, pp. 262-268.
35. Zong, ZM, Zhang, JW, Wang, TX, Xie, RL, Ding, MJ, Cai, KY, Huang, YG, Gao, JS, Wu, YQ & Wei, XY 2007, 'Reactivities of Shenfu chars towards gasification with carbon dioxide', *Journal of China University of Mining and Technology*, vol, 17, no. 2, pp. 197-200.